Princeton Plasma Physics Laboratory

PPPL- 4841

PPPL- 4841

Physics of Radiation-driven Islands Near the Tokamak Density Limit

D.A. Gates, L. Delgado-Apricio and R.B. White

January, 2013

PPPL PRINCETON PLASMA PHYSICS LABORATORY

Prepared for the U.S. Department of Energy under Contract DE-AC02-09CH11466.

Princeton Plasma Physics Laboratory
Report Disclaimers

Full Legal Disclaimer

Trademark Disclaimer

PPPL Report Availability

Princeton Plasma Physics Laboratory:

http://www.pppl.gov/techreports.cfm

Office of Scientific and Technical Information (OSTI):

http://www.osti.gov/bridge

Related Links:

U.S. Department of Energy

Office of Scientific and Technical Information

Fusion Links

Physics of radiation-driven islands near the tokamak density limit

D. A. Gates, L. Delgado-Aparicio, R. B. White

[1]Princeton Plasma Physics Laboratory, Princeton, NJ 08543 USA

Abstract

In previous work [1], the onset criterion for radiation driven islands [2] in combination with a simple cylindrical model of tokamak current channel behavior was shown to be consistent with the empirical scaling of the tokamak density limit [3]. A number of the unexplained phenomena at the density limit are consistent with this novel physics mechanism. In this work, a more formal theoretical underpinning, consistent with cylindrical tearing mode theory, is developed for the onset criteria of these modes. The appropriate derivation of the radiation-driven addition to the modified Rutherford equation is discussed. Additionally, the ordering of the terms in the MRE is examined in a regime near the density limit. It is hoped that given the apparent success of this simple model in explaining the observed global scalings will lead to a more comprehensive analysis of the possibility that radiation driven islands are the physics mechanism responsible for the density limit. In particular, with modern diagnostic capabilities detailed measurements of current densities, electron densities and impurity concentrations at rational surfaces should be possible, enabling verification of the concepts described above.

1. Introduction

Due to the strong dependence of fusion power on plasma density the tokamak density limit has been the subject of intense international study over several decades [3, 4, 5, 6, 7, 8]. As a

result of this effort an agreed upon empirical scaling, referred to as the Greenwald limit [3],

$$\bar{n_e} < \frac{I_p}{\pi a^2} \tag{1}$$

has been developed and extensively verified against international databases. Here, $\bar{n_e}$ is the line averaged (as from an interferometer) electron density, I_p is the total plasma current, and a is the plasma geometric minor radius. The expression in cited in Equation (1) is a surprisingly robust experimental result. The tokamak database covers approximately 2 orders of magnitude in density and current. The phenomenology at the limit is also surprisingly robust. As the density increases towards the limit, there is an increase in edge radiation, followed by a peaking of the current profile which is usually parameterized by the normalized internal inductance, l_i. When the density reaches the limit, a low-order tearing mode, usually of poloidal mode number $m = 2$ and toroidal mode number $n = 1$, appears and causes the plasma to disrupt. The traditional explanation for the appearance of the $m = 2/n = 1$ is that the peaking of the current profile causes the classical tearing parameter, Δ' to become positive. Whereas the trend of greater classical linear instability is correct, it has proved difficult to generate a robust disruptive mechanism based on classical linear instability.

There are several important previously unresolved issues associated with the density limit phenomenology:

1) The scaling is universal, but the density limit appears associated with radiative collapse which can be complicated given the quantum nature of impurity line radiation.

2) If the physics is associated with radiative collapse, why is the density limit so weakly dependent on heating power?

3) Why is the limit only weakly dependent on Z_{eff}?

4) The collapse is associated with the onset of magnetic islands, so why does the limit not depend on plasma shaping which is known to affect MHD stability?

5) Why is the density limit power scaling different in stellarators?

6) Why are tearing modes associated with the radiative collapse?

In this paper we will:

1) propose a simple criteria for the onset of radiation driven islands in the absence of strong island heating,

2) develop a simple model that qualitatively and quantitatively relates the local island onset criteria to the observed global empirical scaling,

3) discuss the cylindrical theory of radiation driven islands, and

4) discuss the properties of the modified Rutherford equation in the vicinity of the density limit.

2. Radiation Driven islands and the Density limit

It has been shown [1] that a simplified onset criteria for radiation driven islands combined with a simple model of the current profile can reproduce the Greenwald density limit scaling. This model is capable of resolving the issues listed in the Introduction. The basic results of this work is repeated here for reference.

The situation for a tokamak island is shown schematically in Figure 1. The problem of heat conduction around a thin island is handled in detail in Reference [9]. We imagine a scenario where an island of small but finite size has been created by a perturbation. Because it is shielded from the auxiliary heating sources, which are typically centrally peaked on the magnetic axis, the stability criterion for radiative driven islands of the island interior is expressed as a constraint

on the radiated power and the ohmic power such that:

$$P_{rad} < \eta J^2 \tag{2}$$

which we rewrite:

$$E_{eff}\nu_{(eZ)_{eff}} n_e < \frac{m_e \nu_{ei}}{e^2 n_e} J^2 \tag{3}$$

where E_{eff} is the energy lost per excitation collision summed over all radiating lines, $\nu_{(eZ)_{eff}}$ is the effective collision frequency for radiative processes, n_e is the electron density, m_e is the electron mass, ν_{ei} is the electron-ion collision frequency, e is the electron charge, and J is the local current density with all quantities evaluated at the rational surface of interest. This expression can be rewritten as:

$$n_e < \sqrt{\frac{m_e}{e^2 E_{eff}} \frac{\nu_{ei}}{\nu_{(eZ)_{eff}}}} J \quad or \quad n_e < f(Z, T_e) J \tag{4}$$

This is suggestive of the Greenwald limit (1). The difference between Equation (4) and Equation (1) is that the island onset criterion (4) is given in terms of local parameters where as the Greenwald limit (1) is in terms of global parameters.

To relate the local parameters of Equation (4) and global parameters of Equation (1) we consider a family of current profiles of the form:

$$J = \frac{J_0}{\left(1 + \left(\frac{r}{r_0}\right)^{2\nu}\right)^{1+\frac{1}{\nu}}} \tag{5}$$

As ν increases, the profiles go from peaked to flat, representing a typical collapsed current profile for large values of ν. This class of profiles was first used in Reference [10]. Additionally

we assume a parabolic density profile. A representative set of current profiles at fixed edge-q is shown in Figure 2. Each curve has J_0 chosen such that $q_0 = 0.9$, consistent with the observation that the peak current density inside the $q = 1$ rational surface is clamped due to the $m/n = 1$ instability (aka the sawtooth instability).

To understand where the Greenwald limit lies in this space we first plot contours of constant total plasma current versus the free profile parameters ν and r_0 (shown in Figure 3). Additional information is required to locate the density limit. In particular, since it is well established that the current profile is peaking as the density limit is approached, a measure of this peaking is required. The required information is taken from a plot from Reference [11]. Figure 6 of this reference shows the operational boundary for the JET tokamak as a function of q_{edge} and l_i. The upper bound of this plot represents the density limit. The limit is parameterized with a linear fit given by:

$$l_i = 0.12 * q_{edge} + 0.6 \tag{6}$$

where l_i is the normalized internal inductance of the plasma (as defined in reference [11]). The contour of the fit curve given by Equation (6) is shown in Figure 3. We note here that for plasmas with high internal inductances as described by the relationship above, plasma boundary shaping does not have a strong effect on the low order rational surfaces so that the shape of these surfaces will be roughly circular. This is a plausible explanation as to why plasma shaping does not affect the Greenwald limit. We also note that the experimentally observed current profile peaking at the density limit corresponds to the knee in the constant q contours where the main variation in the profile parameters changes from strongly varying r_0 to strongly varying ν. This corresponds to the point where the bulk of the (fixed) plasma current is now inside the q=1

surface. Further increase in l_i from this point leads to rapid reductions in the current density outside the $q = 1$ surface. This behavior is important in understanding the relationship between the average current density (which appears in the Greenwald limit) and the current density at a local surface (which appears in the island onset criterion).

The next step is to see if the local criterion due to the onset of a radiation driven island actually corresponds with the Greenwald limit. In other words, along the contour that represents the current profiles for the density limit in Figure 3 there should be a correlation with the following expressions

$$\frac{f(Z)J(r_{m/n})}{n_e(r_{m/n})} = \frac{I_p}{\overline{n}_e \pi a^2} \tag{7}$$

where we have noted the near temperature independence of the quantity $f(Z, T_e)$ as was first noted in Reference [12]. The assumption of a parabolic density profile $n(r) = n(0)(1-(r/a)^2)$ gives:

$$\frac{J(r_{m/n})}{I_{tot}(1-\frac{r_{m/n}^2}{a^2})} = \frac{n_e(0)}{\overline{n}_e}\frac{1}{f(Z)\pi a^2} \tag{8}$$

where the term on the right is constant for the purposes of this discussion.

As an example, the contour of the expression above for the $q = 2$ surfaces as determined by the profile model is shown in blue in Figure 3. The agreement between the observed experimentally determined current profile behavior and the behavior of the radiation driven onset criterion is remarkable given the simplicity of the model used to describe the profile behaviors.

3. Modified Rutherford Equation

The radiation drive effect is best understood in the context of the non-linear island evolution

equation, typically referred to as the modified Rutherford equation (MRE). A version of the equation including the term associated with radiation has been derived [13] and used to model the evolution of the radiation driven islands observed at the density limit. The model used can be written:

$$\frac{k_0}{\eta}\frac{dw}{dt} = \Delta' r_s + C_1 w \tag{9}$$

where the coefficient C_1 is defined by $3(r_s/s)(\delta P/n_e\chi_\perp T_e)$. The onset criteria for the radiation driven tearing mode is satisfied when the RHS of Equation (9) becomes positive.

First we examine the term C_1. In Reference [13] the coefficient was taken from the derivation of the magnitude of the perturbed current density as derived in Reference [2]. We repeat that derivation for reference here, since Reference [2] is not available online. The Δ' term can be derived from three basic relationships: 1) Power balance across island flux surfaces, 2) Ohm's law, and 3) the definition of Δ' for a known helical current perturbation. These condition can be written:

$$\int\int_S n_e\chi_\perp \nabla T_e \, dA = \int\int\int_V \delta P \, dV \tag{10}$$

$$\frac{\delta J}{J} = -\frac{3}{2}\frac{\delta T_e}{T_e} \tag{11}$$

$$\Delta' = 16k_1\frac{\delta J}{swJ} \tag{12}$$

where we have ignored the effects of finite parallel conductivity and s is the shear, k_1 is a constant, and w is the island width. In reference [2] Equation (10) is approximated as:

$$\nabla T_e \sim \frac{\delta P}{n_e \chi_\perp} \frac{V_{island}}{A_{island}} \sim \frac{\delta P}{2 n_e \chi_\perp} w \tag{13}$$

Where V_{island} is the volume A_{island} is the enclosing surface area of the annular torus of the inscribed island. Additionally, the approximation $\nabla T_e \sim 2T_e/w$ is made.

Combining Equations (13), (11), and (12) one finds:

$$\Delta' = 3 \frac{r_s s_I}{s_q} \frac{\delta P}{n_e \chi_\perp T_e} w \tag{14}$$

The approximation used to develop Equation (13) is quite crude. It is often referred to as the "belt model" wherein the island is treated as an annular toroidal ring. The geometric contribution to the error in of the "belt model" approximation can be estimated by assuming the radiation is independent of temperature and that $\chi_\perp$ is a constant across the island. In Figure 4 the curve represented by the ratio the integrals in Equation (10) is compared to the curve generated by the approximation represented in Equation (13). As can be seen in the Figure, there is a substantial error (more than a factor of four in the peak value) associated with the geometric approximations made in Reference [2]. In future work the effect of the temperature dependence of the radiation rate and of the cross-field diffusivity $\chi_\perp$ will also be investigated.

4. Analysis of the MRE

In order to understand the expected behavior of radiation driven islands near the density limit the individual terms in Equation (9) are now considered for parameters that are typical of experimental conditions in the vicinity of the limit. There are several constraints on the problem which require consideration. In particular, the radiated power and the current profile are constrained by the considerations in Section 2. These constraints effectively determine the

island behavior at the density limit.

Classical Δ'

In order to understand the effect of varying Δ' we again return to the high aspect ratio tokamak model adopted in Reference [1]. We calculate Δ' for current profiles along the upper bound of the density limit operational diagram (see Figure 3). The current profiles at the density limit boundary are shown in Figure 5, which have been chosen according to the same criterion in Equation (6). Δ' is calculated according to the method described in reference [15]. The result of this calculation is shown in Figure 6. As can be seen in the figure Δ' crosses through zero as the plasma current is increased. In addition, Δ' is small in absolute value. Typically, in studying non-linear tearing mode phenomena it is assumed without justification that $\Delta' = -2m$ (the vacuum value) for $m > 2$ and $\Delta' = -m$ for $m = 2$. However, for the case in question, since the classical tearing parameter has been postulated as the cause of the onset of the tearing instability observed at the density limit, we have calculated Δ' using the original high aspect ratio circular cross-section formula. It is a well known result that as classical tearing modes grow there is a stabilizing non-linear term as shown in Reference [16]. This island saturation non-linearity has also been calculated, with the results shown in Figure 7. From the figure it can be seen that the non-linearity is important, at least for the class of profiles considered here. The saturated island width (as defined in reference [16]) is the island width at which the classical Δ' goes to zero. As is seen in the Figure, Δ', which is initially small and positive, goes to zero for relatively small islands. We also note that there are additional stabilizing effects that reduce the classical instability that is seen for the 2/1 mode in this model (see for example Reference [17]).

Radiation term

We now consider the coefficient C_1 in Equation (9). The sign of this term varies from

negative to positive as the radiated power density increases, changing sign when the radiated power exceeds the ohmic heating power (when δP changes sign). This is the criteria that led to equation (3). The radiation driven Δ', when negative, will act to reduce the saturated island width that is achieved due to the classical Δ'. When it becomes positive, then the mode is always unstable for all values of w. Given the situation we have described there is no critical island width for mode onset, since there is always a small island present. We note that in order to do quantitative analysis of the actual saturated island widths we should use measured profiles and actual impurity radiation concentrations. There is another important non-linearity associated with the order-of-magnitude reduction in cross-field diffusivity inside an island first reported in reference [18], which will strongly enhance the insulation quality of the islands and will increase the radiation island drive effect.

If we reformulate the second term in Equation (9) as follows:

$$C_1 w = K_1 * \left(\frac{r_s}{sa}\right)\left(\frac{\delta P}{0.1 n_e T_e}\right)\left(\frac{a^2}{\chi_{\perp_{eff}}}\right)\left(\frac{w}{a}\right) \sim 10 K_1 * \left(\frac{r_s}{sa}\right)\left(\frac{w}{a}\right)\left(\frac{\delta P}{P_{tot}}\right) \qquad (15)$$

Where we have made use of the experimental observation that the cross field diffusivity inside and island is approximately and order of magnitude lower than in the bulk plasma [18]. If we make the following estimates:

$$\left(\frac{r_s}{sa}\right) \sim \frac{1}{4} \quad \left(\frac{w}{a}\right) \sim 0.02 \quad \left(\frac{\delta P}{P_{tot}}\right) \sim 0.4 \qquad (16)$$

we find $C_1 \sim 0.02 K_1$. If we use $K_1 = 3$ then thereadiation driven island term would only become important for very small values of Δ'. However, if $K_1 = 12$ according to the effects discussed above then the radiation term is competitive a small but negative value of Δ'. Addition of the temperature dependence of the radiation will further increase the size of the radiation-

driven term.

5. Summary

Experimental evidence [13, 14, 19, 20, 21, 22, 23] has increasingly supported the notion that radiation effects are important in determining the evolution of magnetic islands in tokamaks. In previous work [1] it was shown that the onset criteria for radiation driven islands is consistent with the empirical scaling of the tokamak density limit. In this paper it was shown that the onset criteria expressed in Reference [1] is consistent with the change in sign of the radiation driven Δ' term in the Modified Rutherford Equation. Additionally, it was shown that for the model profiles considered that the classical Δ' is small and positive (indicating a small saturated island). In the model case this would correspond to pure instability with no threshold island. Since the model is approximate, the relative magnitude of the radiation term was considered for reasonable threshold island widths and the radiation drive was found to be sufficiently large to compete with the classical Δ' term, even if the classical term were small and negative. The model predicts a simple testable criteria for mode onset in terms of the local power balance at the rational surface. It is hoped that the apparent success of this theory in explaining the phenomenology of the density limit will lead to direct experiments to test the hypothesis that the radiation driven islands are the origin of the Greenwald limit.

References

[1] D. A. Gates and L. Delgado-Aparicio, Phys. Rev. Letters **108** (2012) 165004.

[2] P. H. Rebut and M. Hugon, Plasma Physics and Controlled Nuclear Fusion Research 1984

(Proc. 10th Int. Conf. London, 1984), Vol. 2, IAEA, Vienna, 197, (1985).

[3] M. Greenwald, J.L. Terry, S.M. Wolfe S. Ejima, M.G. Bell, S.M. Kaye, G.H. Neilson, Nucl. Fusion **28** (1988) 2199.

[4] M. Murakami, J. D. Callen, L. A. Berry, Nucl. Fusion **16** (1976) 347.

[5] S.J. Fielding, J. Hugill, G.M. McCracken, J.W.M. Paul, R. Prentice, P.E. Stott, Nucl. Fusion **17** (1977) 1382.

[6] M. Greenwald, Plasma Phys. Control. Fusion **44** (2002) R27.

[7] R. Granetz, Phys. Rev. Lett. **49** (1982) 658.

[8] E. S. Marmar, J. E. Rice, J. L. Terry, and F. H. Sequin, Nucl. Fusion **22**, 1567 (1982).

[9] R. Fitzpatrick, Phys. Plasmas **2** (1995) 825.

[10] H. P. Furth, P. H. Rutherford, and H. Selberg, Phys. Fluids **16** (1973) 1054.

[11] J. A. Wesson, R. D. Gill, M. Hugon, F. C. Schuller, J. A. Snipes, et al., Nucl. Fusion **29** (1989) 641.

[12] F. W. Perkins and R. A. Hulse, Phys. Fluids **28** (1985) 1837.

[13] F. Salzedas, F. C. Schuller, A.A.M. Oomens, and the RTP Team, Phys. Rev. Lett. **88** (2002) 075002-1.

[14] L. Delgado-Aparicio, D. Stutman, K. Tritz, F. Volpe, K.L. Wong, et al., Nucl. Fusion **51** (2011) 083047.

[15] H. P. Furth, J. Killeen, and M. N. Rosenbluth, Phys. Fluids **6**, 459 (1963).

[16] R. B. White, D. A. Monticello, M. N. Rosenbluth, and B. V. Waddell, Phys. Fluids **20**, 800 (1977).

[17] D. Meshcheriakov, P. Maget, H. Ltjens, P. Beyer, and Xavier Garbet, Phys. Plasmas 19, 092509 (2012).

[18] K. Ida, K. Kamiya, A. Isayama, Y. Sakamoto, and JT-60 Team, Phys. Rev. Lett. **109**, 065001 (2012).

[19] W. Suttrop, K. Buchl, J.C. Fuchs, M. Kaufmann, K. Lackner, et al., Nucl. Fusion, **37** (1997) 119.

[20] B. Esposito G. Granucci, P. Smeulders, S. Nowak, J. R. Martin-Solis, L. Gabellieri, et al., Phys. Rev. Lett. **100** (2008) 045006

[21] L. Delgado-Aparicio, et al., submitted to Phys. Rev. Letters, (2012).

[22] L. Delgado-Aparicio, et al., paper EX/P4-14 at this conference. Proceedings of the 24th IAEA Fusion Energy Conference, San Diego, USA, (2012).

[23] L. Delgado-Aparicio, et al., submitted to Nuclear Fusion, (2012).

Figure Captions

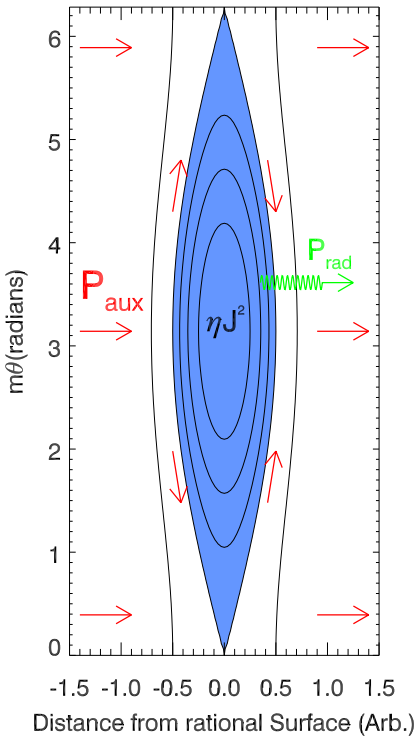

Figure 1: Representation of single lobe of a magnetic island schematically showing the heat flow from the auxiliary heating around the island (red arrows), the resistive heating inside the island (blue area), and the radiation losses from within the island interior (green arrow).

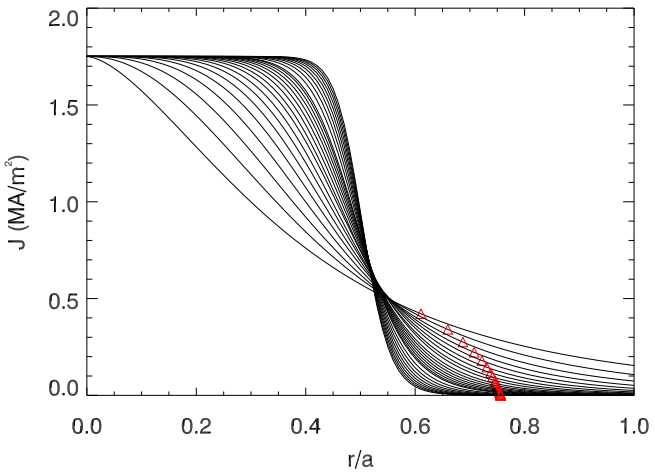

Figure 2: Plot of the family of current density curves used for the density limit model. This set of curves have constant $q_{edge} = 3.5$. The red triangles indicate the position of the q=2 surface for each profile.

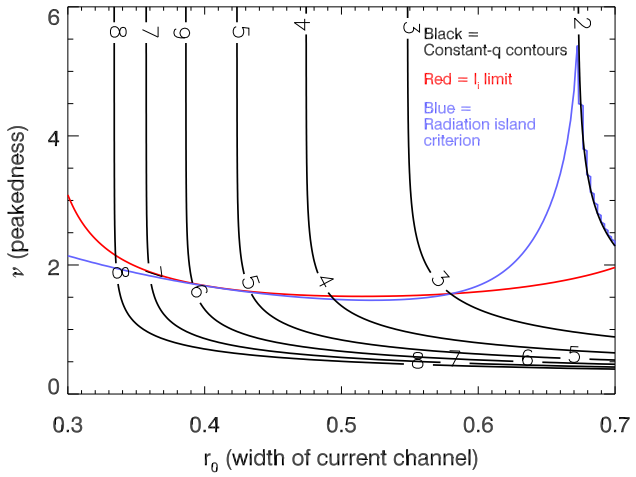

Figure 3: Contour plot of edge q_a (black) as a function of the profile parameters ν and r_0 for $3 < q_a < 8$ in steps of 1. Also shown in the plot are the contour of the current profile peaking corresponding to the density limit as given by Equation (6) (red) and the best fit contour of the island onset criteria from Equation (8) (blue). The correspondence of the red and the blue curve indicate that the island onset criteria coincides with the experimentally observed current profiles at the Greenwald limit.

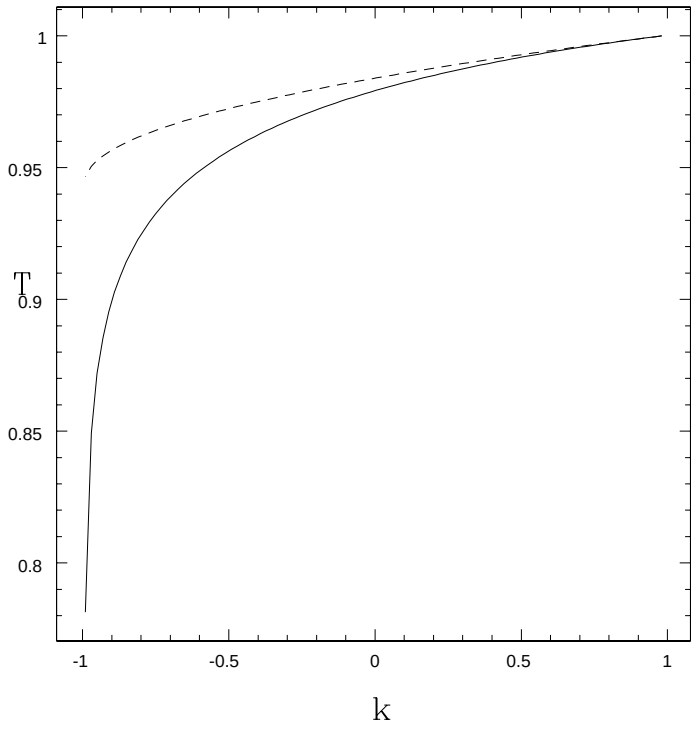

Figure 4: A plot of the electron temperature normalized to the value at the island separatrix. The two curves correspond to a) the exact integral of the of the geometric contribution of the cross-field heat flux reaching the center of the island (solid line) and b) the approximate expression developed in Reference [2] (dashed line). The profiles are plotted vs. the island flux parameter $k = 8(r - r_s)^2/w^2 - 1$ (at the island O-point)

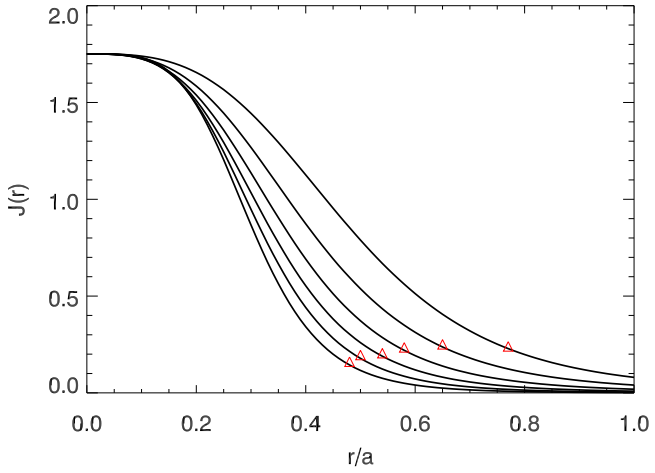

Figure 5: Figure showing the current profiles at the density limit boundary as determined by the relationship in Equation (6). The curves are for $q_a = 3 - 8$ in steps of 1. The red triangles represent the location of the $q = 2$ surface.

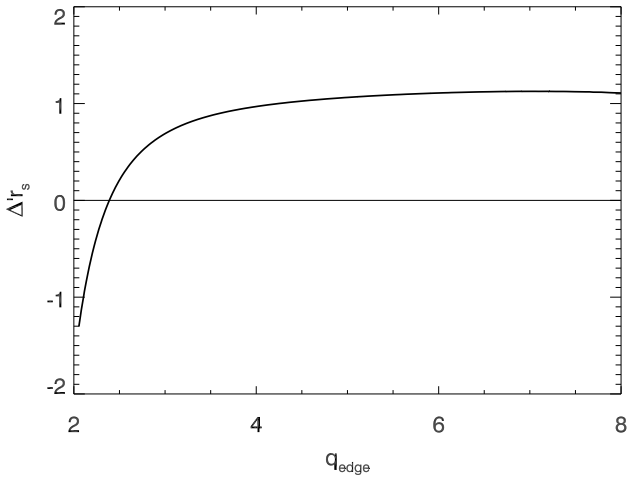

Figure 6: Figure showing the dependence of the classical tearing parameter Δ' as a function of edge q for the class of profiles identified as being at the density limit.

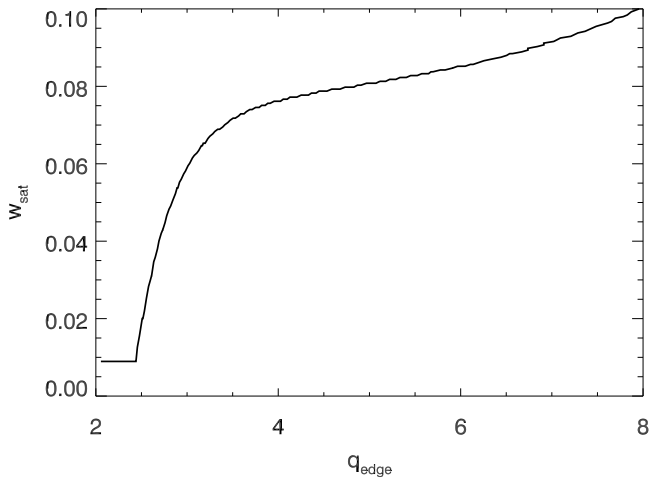

Figure 7: Figure showing the saturated island width (normalized to minor radius) expected for the profiles identified as being at the density limit.

The Princeton Plasma Physics Laboratory is operated
by Princeton University under contract
with the U.S. Department of Energy.

Information Services
Princeton Plasma Physics Laboratory
P.O. Box 451
Princeton, NJ 08543

Phone: 609-243-2245
Fax: 609-243-2751
e-mail: pppl_info@pppl.gov
Internet Address: http://www.pppl.gov